Original Article

MOLECULAR METABOLISM

# Endothelin receptor B-deficient mice are protected from high-fat diet-induced metabolic syndrome

**Martina Feger [1], Leonie Meier [1], Jörg Strotmann [1], Miriam Hoene [2], Julia Vogt [1], Alexandra Wisser [1], Susanna Hirschle [1], Marie-Jo Kheim [1], Berthold Hocher [3,4,5], Cora Weigert [2,6,7], Michael Föller [1,*]**

## ABSTRACT

**Objective:** Endothelin receptor B (ETB) together with ETA mediates cellular effects of endothelin 1 (ET-1), an autocrine and endocrine peptide produced by the endothelium and other cells. It regulates vascular tone and controls kidney function. Metabolic syndrome is due to high caloric intake and is characterized by insulin resistance, dyslipidemia, and white adipose tissue (WAT) accumulation. ETA/ETB antagonism has been demonstrated to favorably influence insulin resistance. Our study explored the role of ETB in metabolic syndrome.
**Methods:** Wild type ($etb^{+/+}$) and rescued ETB-deficient ($etb^{-/-}$) mice were fed a high-fat diet, and energy, glucose, and insulin metabolism were analyzed, and hormones and lipids measured in serum and tissues. Cell culture experiments were performed in HepG2 cells.
**Results:** Compared to $etb^{+/+}$ mice, $etb^{-/-}$ mice exhibited better glucose tolerance and insulin sensitivity, less WAT accumulation, lower serum triglycerides, and higher energy expenditure. Protection from metabolic syndrome was paralleled by higher hepatic production of fibroblast growth factor 21 (FGF21) and higher serum levels of free thyroxine (fT4), stimulators of energy expenditure.
**Conclusions:** ETB deficiency confers protection from metabolic syndrome by counteracting glucose intolerance, dyslipidemia, and WAT accumulation due to enhanced energy expenditure, effects at least in part dependent on enhanced production of thyroid hormone/FGF21. ETB antagonism may therefore be a novel therapeutic approach in metabolic syndrome.


**Keywords** Insulin; Triglyceride; Thyroid hormone; FGF21

**Significance statement**

We found that rescued endothelin receptor B (ETB)-deficient mice were protected from high-fat diet-induced glucose intolerance and insulin resistance, white adipose tissue accumulation, and dyslipidemia compared to wild type mice. These effects were paralleled by higher energy expenditure and enhanced hepatic production of fibroblast growth factor 21 (FGF21) and thyroid hormone T4, factors implicated in the control of energy metabolism, in ETB-deficient mice. Since endothelin receptor antagonism is an established therapy in various human diseases, our findings may be of medical relevance and can lead to novel therapies in metabolic syndrome.

## 1. INTRODUCTION

Endothelin 1-3 (ET-1-3) are peptide hormones and autocrine factors mainly produced in the endothelium, but also by other cells including kidney cells, neurons, or macrophages [1]. In the blood vessels, endothelium-derived ET-1 may have opposing effects depending on the receptors involved. Typical receptors for ET-1 are endothelin receptor A (ETA) and endothelin receptor B (ETB), both being G protein-coupled [1]. ETA stimulation results in vasoconstriction, ETB stimulation in enhanced NO formation, thus favoring vasodilation [2]. In the kidney, ET-1 inhibits $Na^+$ reabsorption, resulting in enhanced urinary excretion of $Na^+$ and water [3]. Whereas complete ETB deficiency is lethal since lack of ETB in the enteric nervous system results in Hirschsprung's disease [4], $etb^{-/-}$ mice with rescued ETB in the enteric nervous system are viable [5]. In line with the role of ETB for NO production, these rescued $etb^{-/-}$ mice suffer from salt-sensitive hypertension [5]. Moreover, they are characterized by enhanced production of fibroblast growth factor 23 (FGF23), a bone-derived hormone that regulates phosphate and vitamin D homeostasis in the kidney [6]. As ETB is required for ET-1 clearance, ETB-deficient mice exhibit high ET-1 serum levels [7].
ET receptors are currently targets in human disease: Bosentan is an ETA and ETB receptor antagonist that is successfully used in the

[1]University of Hohenheim, Department of Physiology, Stuttgart, Germany [2]Institute for Clinical Chemistry and Pathobiochemistry, Department for Diagnostic Laboratory Medicine, University Hospital Tübingen, Tübingen, Germany [3]University of Heidelberg, Department of Nephrology, Mannheim, Germany [4]Institute of Medical Diagnostics, IMD, Berlin, Germany [5]Clinical Research Center for Reproduction and Genetics in Hunan Province, Reproductive and Genetic Hospital of CITIC-Xiangya, Changsha, Hunan, China [6]Institute for Diabetes Research and Metabolic Diseases of the Helmholtz Zentrum München, University of Tübingen, Tübingen, Germany [7]German Center for Diabetes Research (DZD), 85784 Neuherberg, Germany

*Corresponding author. E-mail: michael.foeller@uni-hohenheim.de (M. Föller).

Received March 10, 2023 • Revision received December 20, 2023 • Accepted December 27, 2023 • Available online 28 December 2023

https://doi.org/10.1016/j.molmet.2023.101868

 

treatment of pulmonary artery hypertension although sole ETB deficiency worsens this condition in rats [8]. Also, in heart failure, either selective ETA or combined ETA/ETB antagonism is beneficial [8]. In chronic kidney disease (CKD), selective ETA antagonists reduce proteinuria and blood pressure while ETB antagonism would rather worsen hypertension [9]. Hence, ETA blockade alone or together with ETB receptor antagonism already plays a decisive role in human disease treatment.

Metabolic syndrome is a medical condition affecting millions of humans worldwide [10]. It is characterized by excess fat storage resulting in obesity, impaired insulin sensitivity leading to type II diabetes, abnormal blood lipids and dyslipidemia, as well has high blood pressure and hypertension [10]. Metabolic syndrome is associated with a high socio-economic burden, increases mortality especially due to cardiovascular diseases and cancer, and is the ultimate consequence of too much food intake along with too little physical activity, in conjunction with other environmental and genetic factors [10].

Fibroblast growth factor 21 (FGF21) is a paracrine and endocrine factor produced in the liver that counteracts the negative changes in metabolism typical of metabolic syndrome [11]. It enhances insulin sensitivity [12], improves dyslipidemia e.g. by reducing serum triglycerides [13], and induces weight loss by stimulating fatty acid oxidation and increasing energy expenditure [14].

Pharmacological antagonism of ETA receptor with atrasentan or dual ETA/ETB antagonism with bosentan have been demonstrated to favorably influence the metabolic profile in high-fat diet-fed mice [15]. Both treatments improve glucose tolerance and dyslipidemia in this mouse model, suggesting a role of ETA and/or ETB in glucose and lipid metabolism [15]. In line with this, ETB-deficient rats exhibit better glucose tolerance than wild type rats, however, their plasma triglyceride levels are not different [16].

In view of the high relevance of the metabolic syndrome and the hints of an association of glucose and lipid metabolism with ETB, we sought to explore the role of ETB for metabolic syndrome. To this end, we fed wild type mice ($etb^{+/+}$) and rescued $etb^{-/-}$ mice a high-fat diet and analyzed glucose and lipid metabolism. Moreover, we aimed to identify the mechanism underlying ETB-dependent regulation of energy metabolism.

## 2. MATERIALS AND METHODS

### 2.1. Animal studies and tissue collection

Animal studies were approved by the authorities of the state of Baden-Württemberg, Germany, and all experimental procedures were conducted in accordance with the federal law for the welfare of animals. Male rescued endothelin receptor B-deficient ($etb^{-/-}$) mice at the age of 8—24 weeks were used for the experiments. Rescued $etb^{-/-}$ mice on a mixed C57BL/6/129 background [17] carry a dopamine b-hydroxylase ETB transgene in the enteric nervous system preventing congenital Hirschsprung's disease [5]. Age-matched wild type ($etb^{+/+}$) breeds of mice with B6129PF2/J background (JAX stock #100903; The Jackson Laboratory, Bar Harbor, ME USA) were used as controls. At least two weeks before starting the high-fat diet (HFD, containing 70 % kcal from fat (#C1090-70; Altromin, Lage, Germany)), mice were fed a purified control diet (#C1000; Altromin). Throughout the study, the animals had free access to food and tap water, and body weight was determined weekly.

After 12 weeks on HFD, mice were sacrificed. Liver, brown adipose tissue, epididymal white adipose tissue, heart, kidney, thyroid, and pituitary gland were harvested and immediately snap-frozen or fixed in 4 % buffered paraformaldehyde. Subcutaneous, epididymal, perirenal/retroperitoneal, mesenteric, and brown fat pads were weighed.

The total number of mice included in this study (n = 23 for each genotype with 1 dropout for each genotype) was subjected to different analyses (blood parameters, tests, tissue analyses upon sacrifice). In particular, since it was not possible to obtain enough blood from a single animal to measure all parameters before sacrifice, the *n* numbers vary for different parameters. This was also inevitable to uphold animal welfare standards. The study design and the *n* numbers for the various tests are depicted in Figure 1A.

### 2.2. Serum biochemistry

Blood specimens were acquired by puncturing the retro-orbital plexus under isoflurane anesthesia. Serum triglycerides and total cholesterol were measured by means of a dry chemistry analyzer (Fuji DRI-CHEM NX500i, Fujifilm, Wiesbaden, Germany). LDL cholesterol was analyzed by using an enzymatic assay (Crystal Chem, Zaandam, Germany). The serum concentration of leptin (Merck Millipore, Darmstadt, Germany), insulin (Crystal Chem), free thyroxine (fT4; Cusabio, Houston, TX, USA), ET-1 (R&D systems, Bio-Techne, Wiesbaden, Germany), and FGF21 (BioVendor, Karasek, Czech Republic) were determined by ELISA kits according to the provided instructions.

### 2.3. Glucose and insulin tolerance tests

For glucose tolerance test (GTT), animals were fasted overnight (14 h) with *ad libitum* access to water. The following morning, mice were given glucose (2 g/kg body weight; glucose 10 % from B. Braun, Melsungen, Germany) intraperitoneally (i.p.). Tail blood was collected before (time 0) and 15, 30, 45, 60, 90, and 120 min after injection for measurement of glucose with a glucometer (ACCU CHEK Guide, Roche, Mannheim, Germany). To examine insulin tolerance (ITT), insulin (1.5 IU/kg body weight; NovoRapid 100 IU/ml, Novo Nordisk, Mainz, Germany) was injected i.p. in 4-h-fasted mice. Blood glucose concentration was determined in a blood drop from the tail vein before (time 0) and after insulin injection as indicated.

### 2.4. Indirect calorimetry and activity

Energy expenditure was determined using an indirect calorimetric system (Oxylet, Panlab, Barcelona, Spain). Mice were placed individually in airtight metabolic cages (Panlab) for 48 h and had free access to HFD and tap water. The first 24 h were considered as acclimation phase, and only the data of the last 24 h were analyzed using Metabolism 2.1.04 software (Panlab). Data are presented as average energy expenditure normalized to body weight (kcal/day/kg0.75) during the light and dark phase. In addition, absolute energy expenditure (kcal/day) was analyzed using analysis of covariance (ANCOVA) with body weight or fat-free mass (FFM) as a covariate [18]. FFM was estimated by subtracting total fat mass from body weight.

Activity of mice was analyzed using the ANY-maze video tracking system, version 5.14 (Stoelting Europe, Dublin, Ireland). Single mice were tracked in their respective cage for three consecutive days (72 h) with 10 positions/second. The day—night cycle was 12 h light and 12 h darkness. Mice had free access to water and HFD. The distance moved was recorded using an IR(infrared)-sensitive CCD camera (model DMKAUC03; The Imaging Source, Charlotte, NC, USA) equipped with an IR-compatible vari-focal objective (Computar Europe, Duesseldorf, Germany). During the dark phase, the cage was illuminated by a 10 W IR-lamp with 940 nm light (Synergy 21, Munich, Germany).

 

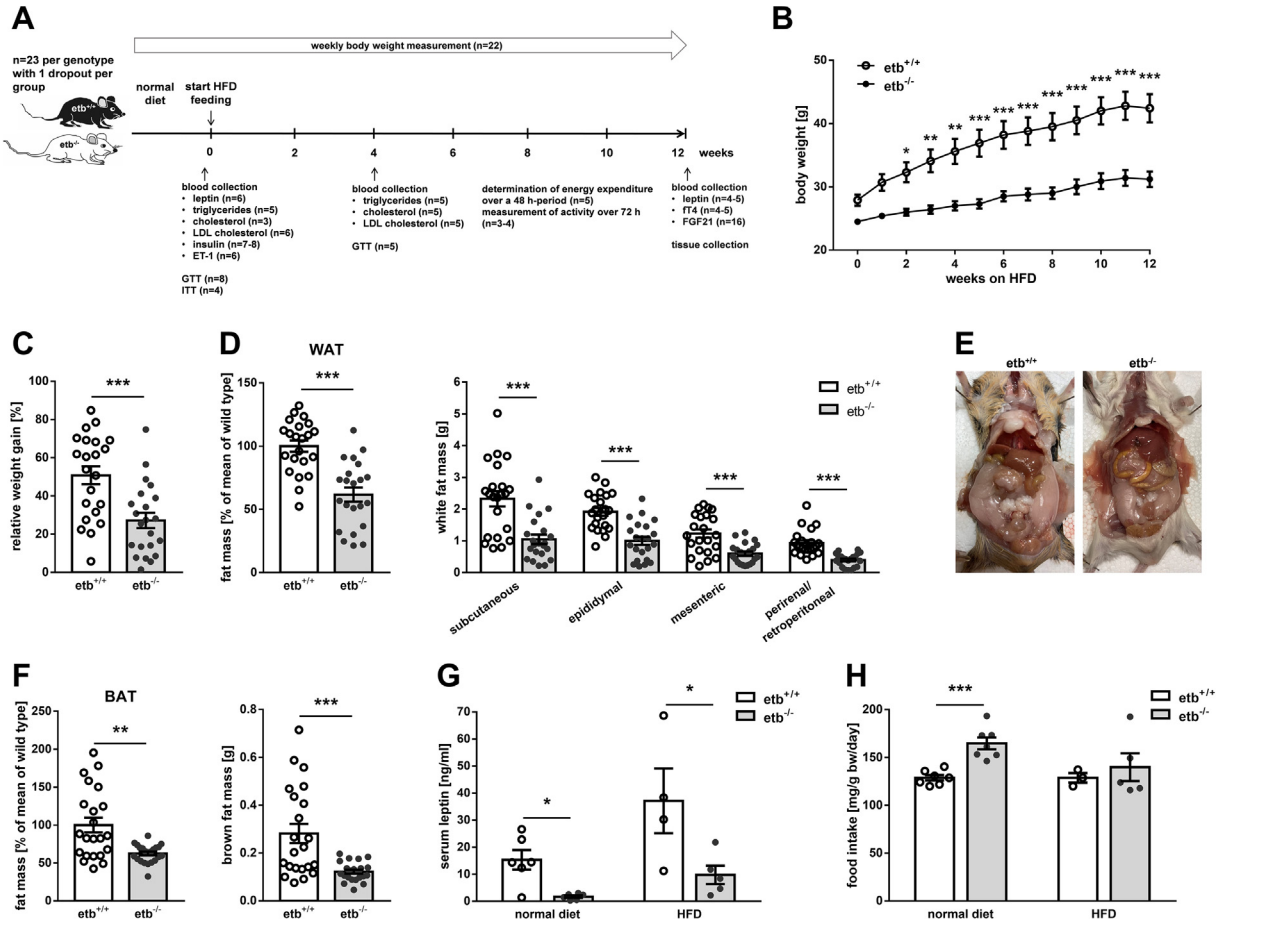


**Figure 1: Lower fat accumulation in ETB-deficient mice than wild type mice following 12 weeks on high-fat diet.** (**A**) Scheme of study design. (**B**) Course of body weight (n = 22 per group) of wild type mice (etb$^{+/+}$) and ETB-deficient (etb$^{-/-}$) mice during 12 weeks of feeding a high-fat diet (HFD). Relative weight gain as percentage (**C**), weight of different fat depots (**D** and **F**: right panels), total white adipose tissue (WAT) (**D**: left panel) and brown adipose tissue (BAT) (**F**: left panel) expressed as percentage of mean of etb$^{+/+}$ mice after 12 weeks on HFD (n = 22 per group for all). (**E**) Photograph of the opened abdomen of an ETB-deficient (etb$^{-/-}$) and a wild type mouse (etb$^{+/+}$) after feeding HFD for 12 weeks. (**G**) Serum leptin concentration before (n = 6 per group) and after (n = 4–5 per group) 12 weeks on HFD. (**H**) Average food intake of etb$^{+/+}$ and etb$^{-/-}$ mice on normal diet (n = 7 per group) or on HFD (n = 3–5 per group). All parameters are given as arithmetic means ± SEM. *$p < 0.05$, **$p < 0.01$ and ***$p < 0.001$ indicate significant difference between the genotypes. (B: two-way ANOVA followed by Bonferroni's post-hoc test for comparison of individual time points; C, D, G and H: two-tailed unpaired Student's *t* test (for F (left panel) and for analysis of serum leptin concertation on normal diet, Welch's correction was applied); F: (right panel): Mann–Whitney U test).

### 2.5. Cell culture experiments

HepG2 cells (#ACC 180; DSMZ, Braunschweig, Germany) were cultured in RPMI-1640 medium supplemented with 10 % fetal bovine serum (FBS), 100 U/ml of penicillin, and 100 μg/ml of streptomycin (all from Gibco, Thermo Fisher Scientific, Karlsruhe, Germany). For the experiments, 350,000 cells were seeded per well in a 12-well plate, grown for 24 h, and then treated with 10 nM 3,3′,5-triiodo-L-thyronine sodium salt (Sigma–Aldrich, Schnelldorf, Germany) for another 24 h. Control cells were incubated with the appropriate volume of vehicle (NaOH).

### 2.6. Quantitative real-time PCR

Total RNA was isolated from mouse pituitary gland, liver, and from human HepG2 cells using peqGold Trifast reagent (VWR, Bruchsal, Germany). Isolated liver RNA was treated with DNase (Thermo Fisher Scientific). RNA extraction from HepG2 cells was followed by DNase treatment and a purification step using the RNase-free DNase Set and RNeasy Mini Kit (both from Qiagen, Hilden, Germany).

Reverse transcription of 1.2 μg of total RNA (or 1.0 μg of total RNA from pituitary gland) was performed using random primers (Promega, Walldorf, Germany) and GoScript Reverse Transcription System (Promega). Quantitative real-time PCR was performed on the CFX Connect Real-Time PCR Detection System (Bio-Rad Laboratories, Feldkirchen, Germany). The final qRT-PCR reaction mix contained 2 μl cDNA template (cDNA from the pituitary gland 1:10 diluted), 10 μl 2x GoTaq qPCR Master Mix (Promega), forward and reverse primers, and sterile water up to 20 μl. The amplification program started with an initial denaturation step at 95 °C for 2 min followed by 40 cycles of denaturation at 95 °C for 10 s, annealing for 30 s and extension at 72 °C for 30 s.

The following primers and primer-specific annealing temperatures were used (5' → 3' orientation):

human *FGF21* (59 °C):
ATCGCTCCACTTTGACCCTG,
GGGCTTCGGACTGGTAAACA;
human *TBP* (59 °C):
TGCACAGGAGCCAAGAGTGAA,

 

CACATCACAGCTCCCCACCA;
mouse *Fgf21* (58 °C):
GGGTGTCAAAGCCTCTAGGT,
CAGGCCTCAGGATCAAAGTGA;
mouse *Gapdh* (58 °C):
GGTGAAGGTCGGTGTGAACG,
CTCGCTCCTGGAAGATGGTG;
mouse *Tbp* (60 °C):
CCAGACCCCACAACTCTTCC,
CAGTTGTCCGTGGCTCTCTT;
mouse *Tshb* (60 °C):
TCAACACCACCATCTGTGCT,
TCTGACAGCCTCGTGTATGC.
mRNA fold changes were calculated by the $2^{-\Delta\Delta Ct}$ method using *Gapdh* or *Tbp* (pituitary tissue and HepG2 cells) as housekeeping genes.

### 2.7. Western Blotting

Liver tissue was lyzed in ice-cold lysis buffer (Tissue Protein Extraction Reagent; Thermo Fisher Scientific) supplemented with complete protease and phosphatase inhibitor cocktail and EDTA (Thermo Fisher Scientific). After centrifugation at 10,000 g and 4 °C for 5 min, proteins were boiled in Roti-Load1 Buffer (Carl Roth, Karlsruhe, Germany). Proteins (30 μg) were separated on SDS polyacrylamide gels and transferred to nitrocellulose membranes. Membranes were incubated overnight at 4 °C with rabbit anti-Fgf21 antibody (diluted 1:1,000; Abcam, Cambridge, UK) and rabbit anti-Gapdh antibody (diluted 1:5,000; Cell Signaling, Frankfurt, Germany) and then with secondary goat anti-rabbit IgG, HRP-conjugated antibody (1:5,000; Cell Signaling) for 1 h at room temperature. Antibody binding was detected with ECL detection reagent, and densitometric analysis was performed using Image Lab software 6.1 (Bio-Rad Laboratories). Data are shown as ratio of Fgf21 protein over loading control Gapdh, normalized to wild type mice ($etb^{+/+}$).

### 2.8. Statistics

Data are presented as mean ± SEM in bar graphs with individual data points unless otherwise indicated, and *n* represents the number of independent cell culture experiments or the number of mice per group, respectively. Shapiro—Wilk test was applied to test for normality. Data were evaluated by one-sample *t* test, two-tailed unpaired Student's *t* test (for data with different standard deviations, Welch's correction was applied), Mann—Whitney U test (for data not normally distributed), or two-way analysis of variance (ANOVA) followed by Bonferroni's multiple comparisons test, as appropriate. Analysis of covariance (ANCOVA) was performed to account for possible confounding effects of body weight or FFM on energy expenditure. Only results with $P < 0.05$ were considered statistically significant. IBM *SPSS Statistics* 27.0 (IBM, Armonk, NY, USA) or GraphPad Prism 6.0 (GraphPad Software Inc., San Diego, CA, USA) were used for statistical analysis.

## 3. RESULTS

In order to investigate the role of endothelin receptor B (ETB) in diet-induced metabolic syndrome, we fed wild type mice ($etb^{+/+}$) and rescued ETB-deficient mice ($etb^{-/-}$) a high-fat diet (HFD) for 12 weeks. Since complete ETB deficiency results in early death due to Hirschsprung's disease (congenital intestinal *aganglionosis*), our $etb^{-/-}$ mice were deficient for ETB in every organ and tissue except for the enteric nervous system to prevent the lethal consequence. These animals were viable and did not exhibit gross abnormalities.

Excess fat storage is a hallmark of metabolic syndrome. Prior to HFD feeding, body weight already tended to be higher in $etb^{+/+}$ than in $etb^{-/-}$ mice (Figure 1B). After HFD initiation, $etb^{+/+}$ mice gained more weight than $etb^{-/-}$ mice (Figure 1B,C). Analysis of adipose tissue mass revealed that $etb^{+/+}$ mice had significantly more white adipose tissue (WAT) than $etb^{-/-}$ after 12 weeks of HFD (Figure 1D, left panel). In fact, WAT mass was 62 ± 7 % ($n = 22$) higher in $etb^{+/+}$ mice compared to $etb^{-/-}$ mice. Analysis of different white fat depots revealed that mass of subcutaneous, epididymal, mesenteric, and perirenal/retroperitoneal were all higher in $etb^{+/+}$ mice than $etb^{-/-}$ mice (Figure 1D, right panel; Figure 1E). Thus, ETB deficiency ameliorated diet-induced WAT accumulation. Also, brown adipose tissue (BAT) mass was significantly higher in $etb^{+/+}$ mice than $etb^{-/-}$ mice (Figure 1F). Liver histology did not reveal overt differences as far as pathologies or fat content is concerned (Suppl. Figure 1). In line with less WAT in $etb^{-/-}$ mice, serum leptin levels were significantly lower in both, normal diet-fed and HFD-fed $etb^{-/-}$ mice compared to $etb^{+/+}$ mice (Figure 1G). Moreover, *Ppargc1a* (encoding PGC1α) gene expression was higher and *Ucp1* gene expression was lower in WAT of $etb^{-/-}$ mice compared to $etb^{+/+}$ mice upon HFD feeding (Suppl. Figure 2A) whereas no difference in expression of these genes was observed in BAT (Suppl. Figure 2B). Histological analysis uncovered smaller adipocytes in WAT from $etb^{-/-}$ mice on HFD compared to $etb^{+/+}$ mice (Suppl Figure 2C). HFD feeding resulted in a higher number of cell nuclei per area in BAT from $etb^{-/-}$ mice than $etb^{+/+}$ mice suggesting less whitening in $etb^{-/-}$ mice (Suppl. Figure 2D).

In theory, reduced WAT mass of $etb^{-/-}$ mice could be due to lower food intake. However, food intake of $etb^{-/-}$ mice on normal diet was significantly larger than food intake of $etb^{+/+}$ mice (Figure 1H). On HFD, food intake still tended to be higher in $etb^{-/-}$ mice than in $etb^{+/+}$ mice (Figure 1H). Taken together, $etb^{-/-}$ mice accumulated significantly less WAT than $etb^{+/+}$ mice when placed on HFD.

Dyslipidemia is another hallmark of metabolic syndrome. Therefore, we analyzed blood lipids in the animals at different time points. Prior to HFD feeding, serum triglycerides were significantly lower in $etb^{-/-}$ mice than $etb^{+/+}$ mice (Figure 2A). After 4 weeks on HFD, serum triglycerides were elevated in both genotypes with levels in $etb^{-/-}$ mice being again significantly lower than in $etb^{+/+}$ mice (Figure 2B). Total serum cholesterol levels (Figure 2C,D) and LDL cholesterol concentration (Figure 2E,F) were, however, not significantly different between $etb^{-/-}$ mice and $etb^{+/+}$ mice neither on normal diet nor after 4 weeks on HFD.

A major manifestation of metabolic syndrome is insulin resistance, resulting in reduced glucose tolerance. We performed intraperitoneal glucose tolerance tests in the animals before and 4 weeks after starting HFD feeding. As demonstrated in Figure 3A, upper panel, glucose tolerance was significantly better in $etb^{-/-}$ mice than $etb^{+/+}$ mice when fed a normal diet. After 4 weeks on HFD, glucose tolerance was impaired in both groups but still significantly better in $etb^{-/-}$ mice than $etb^{+/+}$ mice (Figure 3A, lower panel). To investigate whether improved glucose tolerance of $etb^{-/-}$ mice is associated with enhanced insulin sensitivity, we performed an insulin tolerance test. As illustrated in Figure 3B, insulin sensitivity was indeed higher in normal diet-fed $etb^{-/-}$ mice than $etb^{+/+}$ mice. We also studied insulin serum levels. In line with better glucose tolerance and insulin sensitivity, serum insulin levels were significantly lower in normal diet-fed $etb^{-/-}$ mice than $etb^{+/+}$ mice (Figure 3C) after 4 h of fasting. Taken together, $etb^{-/-}$ mice were characterized by better glucose tolerance and higher insulin sensitivity than $etb^{+/+}$ mice.

 

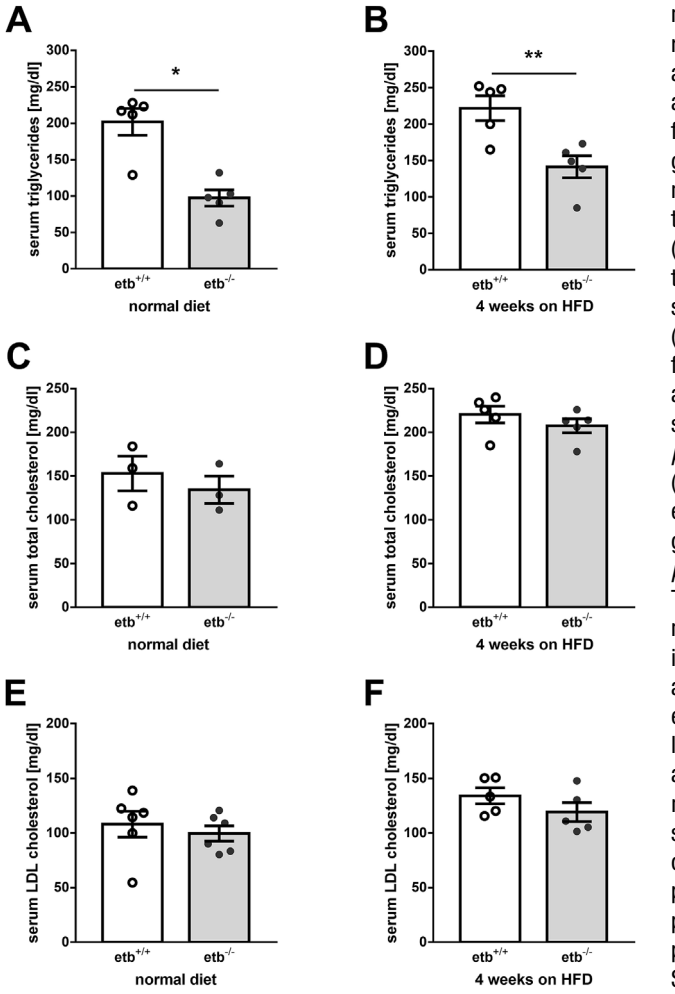


**Figure 2: ETB deficiency results in lower serum triglyceride levels.** Arithmetic means ± SEM of serum concentrations of triglycerides (**A** and **B**; n = 5 per group for both analyses), total cholesterol (**C**; n = 3 per group and **D**; n = 5 per group), and LDL cholesterol (**E**; n = 6 per group and **F**; n = 5 per group) in wild type mice ($etb^{+/+}$) and $etb^{-/-}$ mice on normal diet (**A**, **C**, **E**) or after 4 weeks on high-fat diet (HFD) (**B**, **D**, **F**). *$p < 0.05$ and **$p < 0.01$ indicate significant difference between the genotypes. (A: Mann Whitney test; B–F: two-tailed unpaired Student's *t* test).

Our results thus far suggest that $etb^{-/-}$ mice exhibited lower WAT accumulation, a better lipid profile and higher glucose tolerance than $etb^{+/+}$ mice. Since these more beneficial metabolic parameters were observed despite higher food intake of $etb^{-/-}$ mice, we measured energy expenditure of the animals. As shown in Figure 4A, energy expenditure normalized to body weight was significantly higher in $etb^{-/-}$ mice than in $etb^{+/+}$ mice, suggesting that ETB deficiency leads to enhanced caloric usage, thereby providing protection from manifestations of diet-induced metabolic syndrome. As illustrated in Figure 4B, energy expenditure was indeed higher in $etb^{-/-}$ mice compared to $etb^{+/+}$ mice at each time point throughout their presence in the metabolic cages that included both, an acclimatization period and the actual measurement period. In view of their higher food intake, enhanced physical activity of $etb^{-/-}$ mice could, at least in theory, account for their higher energy expenditure, in particular if higher energy expenditure is mostly, if not exclusively observed at night. However, separate analysis revealed higher energy expenditure of $etb^{-/-}$ mice both, at day (as an estimation of resting energy expenditure) and at night (during activity) (Figure 4C). In line with this, physical activity as estimated from the distance moved was not significantly different between the genotypes (Figure 4D). Also, absolute energy expenditure without normalization to body weight was significantly higher in $etb^{-/-}$ mice than $etb^{+/+}$ mice (Suppl. Figure 3A). If normalized to fat-free mass (FFM), energy expenditure still tended to be higher in $etb^{-/-}$ mice than $etb^{+/+}$ mice, a difference, however, not reaching statistical significance (Suppl. Figure 3C). Additionally, analysis of covariance (ANCOVA) was performed to account for possible confounding effects of body weight or FFM on total energy expenditure. After adjusting for body weight, total energy expenditure was still significantly different between the genotypes, $F(1,7) = 10.799$, $p = 0.013$, partial $\eta^2 = 0.607$ (with $p = 0.166$ for body weight) (Suppl. Figure 3B). After adjusting for FFM, the difference in total energy expenditure was also statistically significant between the genotypes, $F(1,7 = 8.329$, $p = 0.023$, partial $\eta^2 = 0.543$ (with $p = 0.256$ for FFM) (Suppl. Figure 3D).

Thyroid hormones T3 and T4 are known to ramp up energy expenditure not least by burning fat. In order to test whether this effect also plays a role in ETB deficiency, we studied free thyroxine (fT4) serum levels in $etb^{+/+}$ and $etb^{-/-}$ mice. As demonstrated in Figure 5A, HFD-fed $etb^{-/-}$ mice exhibited significantly higher fT4 serum levels than $etb^{+/+}$ mice, an effect likely to contribute to their higher energy expenditure and lower WAT accumulation. In order to analyze whether hyperthyroidism of $etb^{-/-}$ mice is primary or secondary, we determined hypophyseal thyroid-stimulating hormone, beta subunit (encoded by *Tshb*) expression by qRT-PCR. As visualized in Figure 5B, *Tshb* expression was rather suppressed in $etb^{-/-}$ mice compared to $etb^{+/+}$ mice, a result in line with primary hyperthyroidism, i.e. ETB deficiency enhanced thyroid hormone production independently of the hypothalamus-pituitary gland axis.

Since thyroid hormones induce FGF21, an endocrine and paracrine factor produced in the liver which also increases energy expenditure and ameliorates glucose tolerance [14], we considered its involvement, too. First, we demonstrated in cell culture experiments with hepatic HepG2 cells that T3 indeed significantly enhances *FGF21* gene expression (Figure 6A). In order to investigate whether hyperthyroidism of $etb^{-/-}$ mice was paralleled by enhanced FGF21 production, we next measured hepatic *Fgf21* transcripts by qRT-PCR. As demonstrated in Figure 6B, $etb^{-/-}$ mice exhibited significantly higher hepatic *Fgf21* expression after 12 weeks of HFD feeding than $etb^{+/+}$ mice. Also, FGF21 protein was significantly more abundant in the livers from $etb^{-/-}$ mice compared to $etb^{+/+}$ mice, as revealed by Western Blotting (Figure 6C). Circulating FGF21 levels were, however, significantly lower in $etb^{-/-}$ mice than $etb^{+/+}$ mice (Figure 6D). Hence, ETB deficiency was associated with enhanced hepatic FGF21 production, an effect expected to contribute to improved hepatic glucose metabolism upon HFD feeding.

ET-1 may directly increase thyroid hormone levels as higher levels of ET-1 are associated with hyperthyroidism [19]. In line with this, $etb^{-/-}$ mice exhibited higher ET-1 serum levels compared to $etb^{+/+}$ mice (Figure 7). In the absence of ETB, higher circulating levels of ET-1 could bind to ETA thereby causing effects associated with the observed beneficial metabolic phenotype. We therefore determined *Ednra* (encoding ETA) gene expression in different tissues. As illustrated in Suppl. Figure 4, *Ednra* gene expression was not significantly different between the genotypes in liver, WAT, and heart, whereas it was slightly, but significantly higher in BAT and kidney from $etb^{-/-}$ mice

 

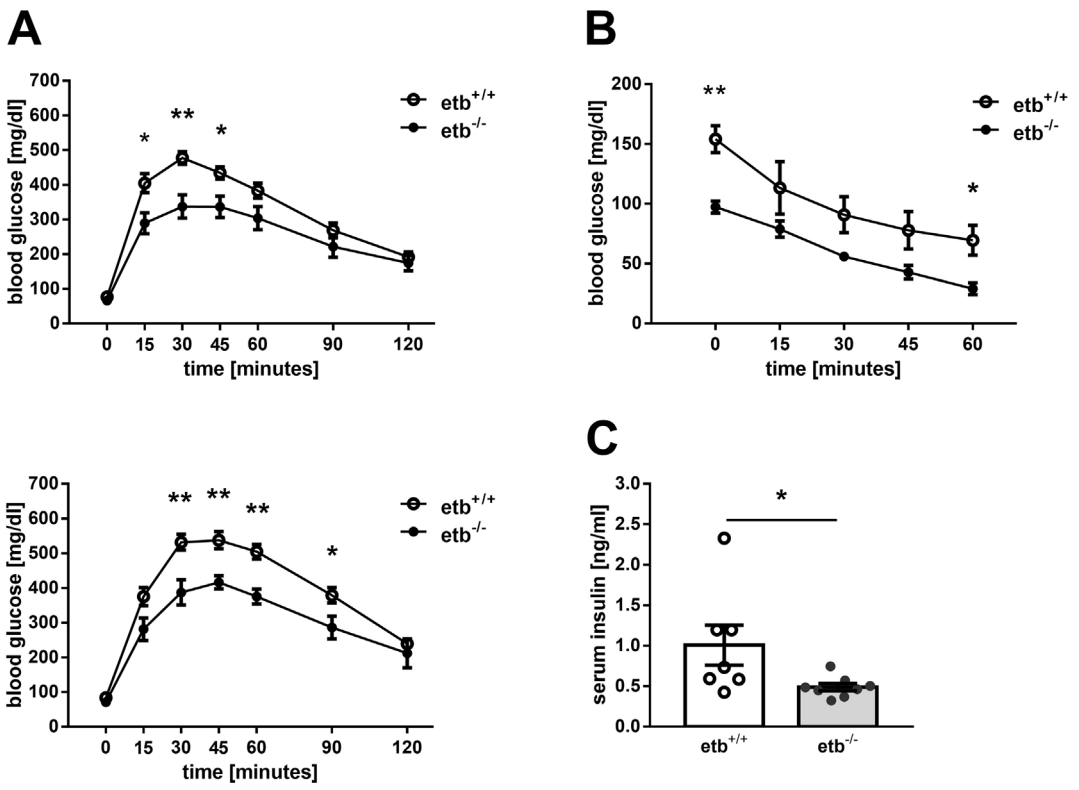


**Figure 3: Improved glucose tolerance and insulin sensitivity in ETB-deficient mice.** (**A**) Time course of blood glucose concentration following i.p. injection of glucose (2 g/kg body weight) in overnight-fasted wild type mice ($etb^{+/+}$) and $etb^{-/-}$ mice before (upper panel; n = 8 per group) and after 4 weeks of feeding a HFD (lower panel; n = 5 per group). (**B**) Time course of blood glucose levels (n = 4 per group) in $etb^{+/+}$ and $etb^{-/-}$ mice on normal diet that had been fasted for 4 h and received an i.p. injection of insulin (1.5 IU/kg body weight). (**C**) Serum insulin levels (n = 7–8 per group) in 4-h-fasted $etb^{+/+}$ and $etb^{-/-}$ mice on normal diet. All parameters are given as arithmetic means ± SEM. $*p < 0.05$ and $**p < 0.01$ indicate significant difference between the genotypes. (A and B: two-tailed unpaired Student's *t* test; C: Mann–Whitney U test).

compared to $etb^{+/+}$ mice. In the thyroid gland from $etb^{-/-}$ mice, it was, however, significantly lower compared to $etb^{+/+}$ mice (Suppl. Figure 4B).

ET-1 and ETB are implicated in pro-inflammatory responses [20,21]. In order to assess the state of inflammation upon HFD feeding, we determined gene expression of *Tnf* (encoding TNFα) and *Il1b* (encoding IL-1β), two pro-inflammatory cytokines implicated in metabolic syndrome, in relevant organs. As depicted in Suppl. Figure 5, both *Tnf* and *Il1b* expression were higher in liver, WAT, and BAT from $etb^{-/-}$ mice compared to $etb^{+/+}$ mice.

Owing to the role of ET-1 and ETB in the cardiovascular system, we also determined parameters of heart and vessel function. Cardiac *Nppb* (encoding brain natriuretic peptide, BNP) expression (Suppl. Figure 6A), a marker of heart failure, and serum asymmetric dimethylarginine (ADMA; Suppl Figure 6B) levels, a marker of endothelial dysfunction, were not significantly different between the genotypes. Cardiac histology revealed a significantly smaller cardiomyocyte diameter in $etb^{-/-}$ mice (Suppl. Figure 6C).

## 4. DISCUSSION

Our investigations revealed that ETB-deficient mice ($etb^{-/-}$) are protected from several hallmarks of metabolic syndrome induced by feeding a high-fat diet (HFD).

Major manifestations of metabolic syndrome are WAT accumulation resulting in obesity, dyslipidemia with high triglyceride and cholesterol levels, decreased insulin sensitivity with glucose intolerance, as well as hypertension [10]. The coincidence of these conditions is particularly common in patients with type II diabetes and is associated with significant sequelae, especially cardiovascular diseases, and increased mortality [10]. Since $etb^{-/-}$ mice *per se* suffer from salt-sensitive hypertension due to the effects of ETB activation on the generation of vasodilator NO [5], we did not study blood pressure in the mice following HFD feeding. However, we provide evidence that ETB deficiency protects from the other three manifestations of metabolic syndrome.

Although $etb^{-/-}$ mice did not exhibit lower food intake, their total WAT mass was markedly and significantly lower following 12 weeks of HFD compared to $etb^{+/+}$. Accordingly, also serum leptin levels were significantly lower in $etb^{-/-}$ mice than in $etb^{+/+}$. These results indicate that ETB deficiency enhanced energy metabolism, a notion corroborated by higher energy expenditure of $etb^{-/-}$ mice compared to $etb^{+/+}$ mice. Energy expenditure turned out to be higher in $etb^{-/-}$ mice than $etb^{+/+}$ mice throughout day and night. Moreover, covariate analysis with FFM as a covariate [18] still yielded higher energy expenditure in $etb^{-/-}$ mice. Finally, physical activity was not significantly different between the genotypes. These results are in line with altered energy metabolism rather than merely enhanced physical activity accounting for higher energy expenditure in $etb^{-/-}$ mice.

Less WAT accumulation in $etb^{-/-}$ mice was paralleled by smaller adipocytes and higher *Ppargc1a* (encoding PCG1α) expression, a finding in line with protection from metabolic syndrome due to hyperthyroidism as PCG1α in WAT confers protection from insulin resistance and promotes mitochondrial biogenesis [22]. A higher

 

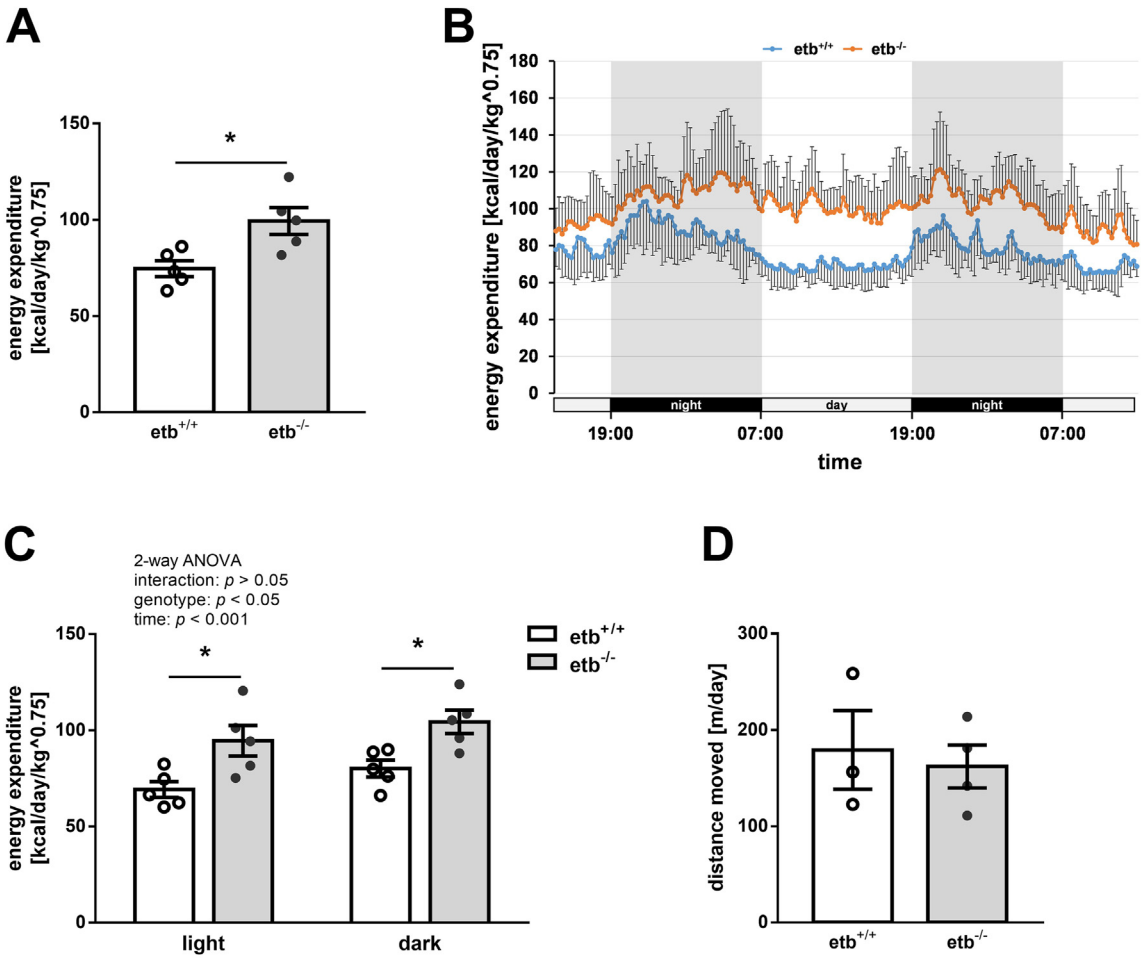


**Figure 4: Enhanced energy expenditure in ETB-deficient mice.** Average total energy expenditure ± SEM (**A**; n = 5 per group), energy expenditure traces (with SD) over the entire 48 h-period (**B**; n = 5 per group), average energy expenditure ± SEM during the light and dark phase (**C**; n = 5 per group), and average distance moved ± SEM (**D**; n = 3–4) of wild type (etb$^{+/+}$) mice and etb$^{-/-}$ mice determined after 6–11 weeks of feeding a high-fat diet (HFD). Note: Figure 4C is a more precise presentation of the results of Figure 4A. *$p < 0.05$ indicates significant difference between the genotypes. (A and D: two-tailed unpaired Student's *t* test; C: two-way ANOVA followed by Bonferroni's multiple comparisons test) standard deviation, SD.

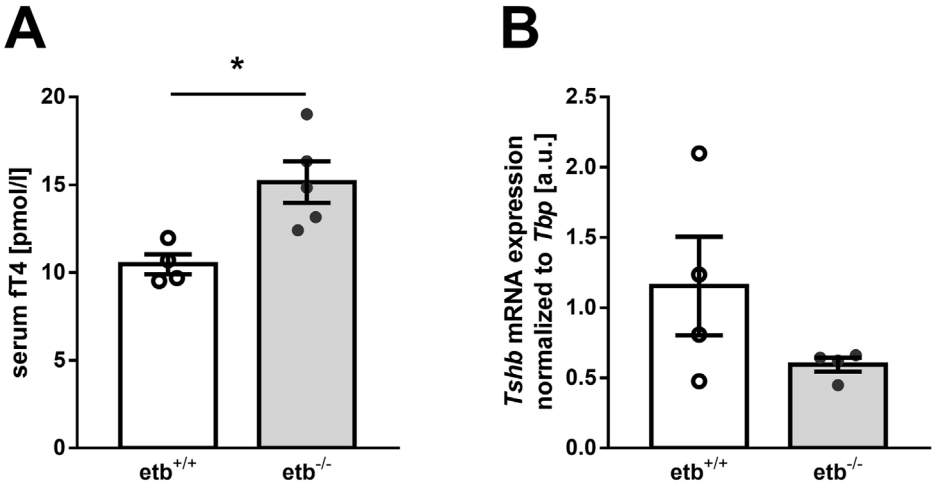


**Figure 5: ETB deficiency results in increased serum concentration of free thyroxine after a 12-week high-fat diet.** Arithmetic means ± SEM of serum concentration of free thyroxine (fT4) (**A**; n = 4–5 per group) and pituitary thyroid-stimulating hormone, beta subunit (encoded by *Tshb*) mRNA expression, normalized to TATA-box binding protein (*Tbp*) (**B**; n = 4 per group) in wild type mice (etb$^{+/+}$) and etb$^{-/-}$ mice fed a high-fat diet (HFD) for 12 weeks. *$p < 0.05$ indicates a significant difference from etb$^{+/+}$ mice. (A: two-tailed unpaired Student's *t* test; B: two-tailed unpaired Student's *t* test with Welch's correction) arbitrary units, a.u.

 

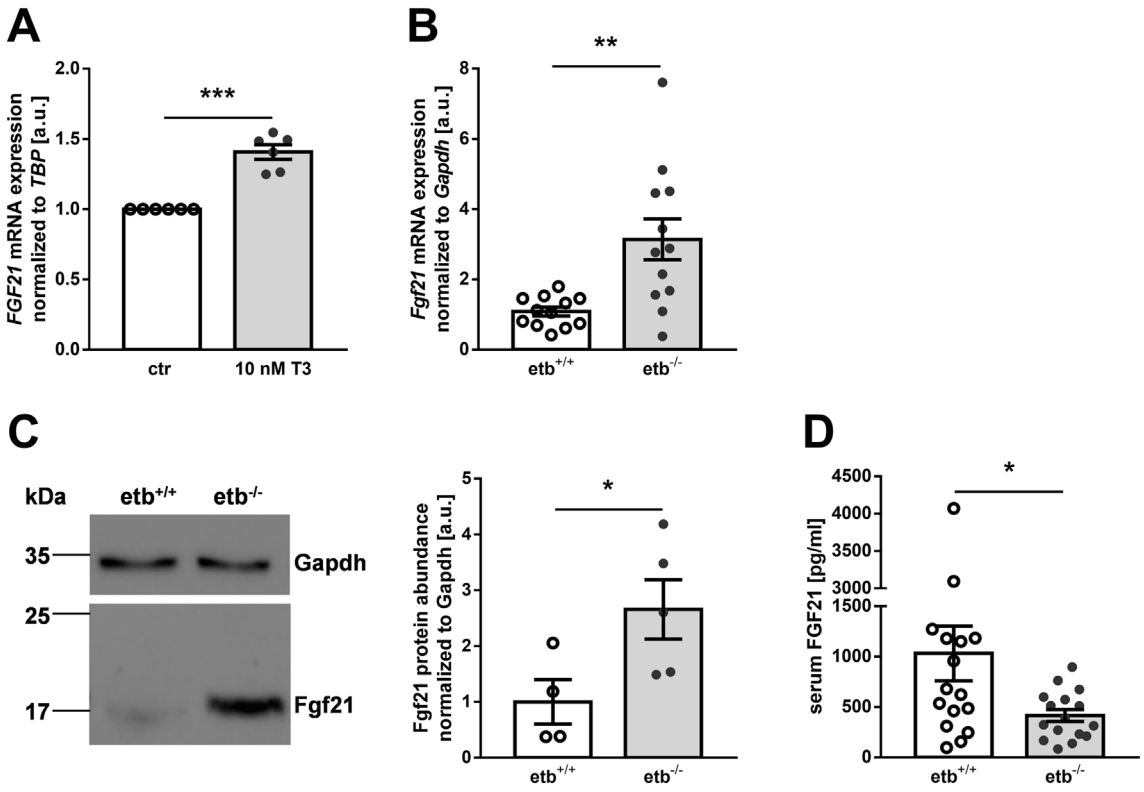


**Figure 6: Enhanced hepatic production of fibroblast growth factor 21 (FGF21) in ETB-deficient mice fed a high-fat diet.** (**A**) Fibroblast growth factor 21 (*FGF21*) mRNA expression, normalized to TATA-box binding protein (*TBP*) in HepG2 cells treated with vehicle control (ctr) or 10 nM 3,3′,5-triiodo-L-thyronine sodium salt (T3) for 24 h (n = 6). (**B**) Hepatic fibroblast growth factor 21 (*Fgf21*) mRNA expression (n = 12 per group), normalized to the housekeeping gene glyceraldehyde-3-phosphate dehydrogenase (*Gapdh*) in wild type mice ($etb^{+/+}$) and $etb^{-/-}$ mice after 12 weeks of feeding a high-fat diet (HFD). (**C**) Representative original Western blot (left panel) and densitometric analysis (right panel) of hepatic Fgf21 protein abundance, normalized to loading control Gapdh (n = 4–5 per group) from $etb^{+/+}$ and $etb^{-/-}$ mice fed a HFD for 12 weeks. (**D**) Serum concentration of FGF21 (n = 16 per group) in $etb^{+/+}$ and $etb^{-/-}$ mice after feeding a HFD for 12 weeks. All data are expressed as arithmetic means ± SEM. $*p < 0.05$, $**p < 0.01$ and $***p < 0.001$ indicate a significant difference from control-treated cells or wild type mice, respectively. (A: one-sample *t* test; B: two-tailed unpaired Student's *t* test with Welch's correction; C: two-tailed unpaired Student's *t* test; D: Mann–Whitney U test) arbitrary units, a.u.

number of cell nuclei per area in BAT from $etb^{-/-}$ mice compared to $etb^{+/+}$ mice suggests that HFD feeding led to less whitening of BAT in $etb^{-/-}$ mice than $etb^{+/+}$ mice. Also this observation supports the notion of ETB deficiency providing protection from metabolic syndrome due to hyperthyroidism. Surprisingly, *Ucp1* gene expression as a proxy of browning was lower in WAT from $etb^{-/-}$ mice than $etb^{+/+}$ mice. Whereas this observation can be expected to compromise protection from metabolic syndrome, it is obviously outweighed in $etb^{-/-}$ mice by the aforementioned factors.

Serum triglyceride levels were significantly lower in $etb^{-/-}$ mice than in $etb^{+/+}$ mice. Hence, ETB deficiency also provided protection from dyslipidemia.

Also, $etb^{-/-}$ mice exhibited better glucose tolerance due to improved insulin sensitivity compared to $etb^{+/+}$ mice. Insulin resistance leading to impaired glucose tolerance characterizes type II diabetes, a leading cause of which is long-term high caloric intake. Higher energy expenditure of $etb^{-/-}$ mice with subsequent fat burning can also be expected to contribute to their better glucose tolerance as chronic inflammation in WAT is a major inducer of insulin resistance [23,24]. Hence, lower WAT mass in ETB deficiency is likely to also account for better insulin sensitivity.

FGF21 is a major hepatic regulator inducing the improvements of energy metabolism that are characteristic of $etb^{-/-}$ mice compared to $etb^{+/+}$ mice: It lowers blood lipids, improves glucose tolerance and centrally stimulates energy expenditure [14]. We indeed found significantly higher hepatic production of FGF21 in $etb^{-/-}$ mice than in $etb^{+/+}$ mice on both, transcriptional and protein level. Therefore, hepatic FGF21 can be expected to make a significant contribution to the better metabolic profile of $etb^{-/-}$ mice compared to $etb^{+/+}$ mice. Surprisingly, circulating FGF21 was lower in $etb^{-/-}$ mice than $etb^{+/+}$ mice. The underlying cause has remained enigmatic in this study. It has to be kept in mind that hepatic production and secretion of FGF21 do not necessarily go hand in hand. In line with this, glucagon induces hepatic FGF21 secretion but suppresses its gene expression [25] while PPARα ramps up both, hepatic FGF21 gene expression and secretion [26]. This shows that stimulation of hepatic FGF21 as observed in this study and FGF21 secretion may be distinct events. Also, our observation of lower circulating FGF21 in $etb^{-/-}$ mice may be misleading due to FGF21's short half-life of only 0.7–1.1 h [27]. Despite the finding of lower circulating FGF21 in $etb^{-/-}$ mice, higher FGF21 hepatic gene expression and protein abundance can at least be expected to significantly contribute to hepatic manifestations of the better metabolic profile upon HFD feeding, e.g. improved glucose metabolism.

Thyroid hormones are classical stimulators of energy expenditure. Higher fT4 serum levels in $etb^{-/-}$ mice compared to $etb^{+/+}$ mice can therefore be expected to also account for their enhanced energy expenditure. Moreover, as suggested by a previous study and

 

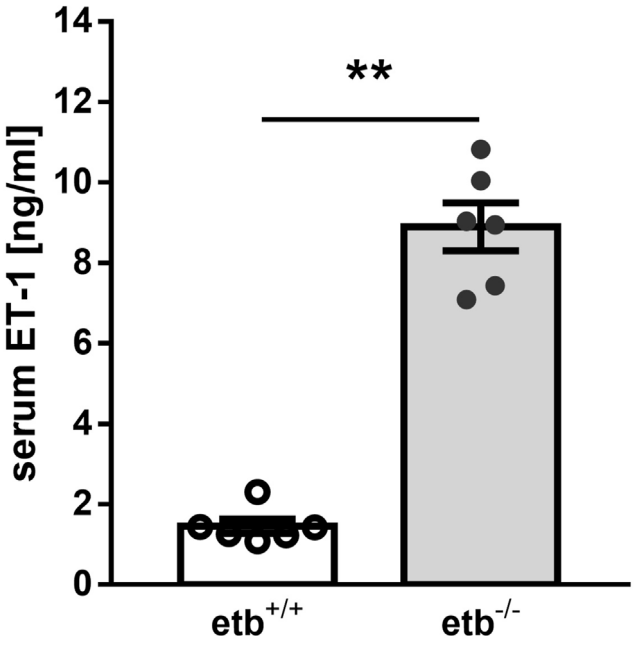


**Figure 7: ETB-deficient mice exhibit elevated serum levels of endothelin 1.** Arithmetic means ± SEM (n = 6 per group) of the serum endothelin 1 (ET-1) concentration in wild type ($etb^{+/+}$) and $etb^{-/-}$ mice on normal diet. $^{**}p < 0.01$ indicates significant difference between $etb^{+/+}$ and $etb^{-/-}$ mice. (Mann–Whitney U test).

demonstrated by our cell culture experiment with hepatic HepG2 cells, thyroid hormones enhance FGF21 production in the liver [28]. Therefore, hyperthyroidism of $etb^{-/-}$ mice is likely to contribute, at least in part, to enhanced FGF21 production in ETB deficiency. Besides, it also up-regulates energy expenditure in an FGF21-independent manner.

We detected rather suppressed hypophyseal TSH expression in $etb^{-/-}$ mice compared to $etb^{+/+}$ mice, a result suggesting primary hyperthyroidism in ETB deficiency, i.e. a thyroid gland-intrinsic mechanism of enhanced hormone production. In a correlation study, ET-1 has been demonstrated to be associated with hyperthyroidism [19], and $etb^{-/-}$ mice had higher ET-1 serum levels since ETB is involved in ET-1 clearance [7]. Hence, it is tempting to speculate that ET-1 enhanced T4 levels in $etb^{-/-}$ mice through ETA. Interestingly, *Ednra* (encoding ETA) expression was significantly lower in the thyroid gland from $etb^{-/-}$ mice than $etb^{+/+}$ mice whereas it was unaltered in all other organs or slightly upregulated in BAT and kidney. It appears to be possible that down-regulated *Ednra* expression in the thyroid gland may be a mechanism to limit ET-1-dependent hyperthyroidism in ETB deficiency.

Inflammation as assessed from *Tnf* and *Il1b* mRNA expression in liver, WAT, and BAT was enhanced in $etb^{-/-}$ mice compared to $etb^{+/+}$ mice. This surprising finding seems to be in contrast to better insulin sensitivity and protection from metabolic syndrome as metabolic syndrome is a pro-inflammatory condition [29]. However, since ET-1 elicits pro-inflammatory responses through ETA [21,30] higher ET-1 levels in $etb^{-/-}$ mice may account for their pro-inflammatory state. Rather, pro-inflammatory cytokines could further enhance energy expenditure in $etb^{-/-}$ mice along with hyperthyroidism [31].

Cardiac *Nppb* mRNA expression, a marker of heart failure, and serum ADMA levels, a marker of endothelial dysfunction, were not different between the genotypes. However, cardiac histology revealed a smaller cardiomyocyte diameter in $etb^{-/-}$ mice, suggesting reduced pressure overload upon HFD feeding. Whereas $etb^{-/-}$ mice do not have hypertension *per se*, they are characterized by endothelial dysfunction [5]. Metabolic syndrome is characterized by hypertension, and HFD feeding indeed elevates blood pressure [32]. In view of these facts, similar cardiac *Nppb* expression and serum ADMA levels and smaller cardiomyocyte diameter in $etb^{-/-}$ mice may therefore be interpreted that ETB deficiency also confers, at least to some extent, protection from hypertension and its negative impact on the cardiovascular system of HFD. It is definitely a limitation of this paper, however, that blood pressure was not measured.

The findings of our study may have a clinical relevance: Blockade of endothelin receptors with specific ETA or dual ETA/ETB antagonists is part of the state-of-the-art treatment of pulmonary hypertension [33] and systemic sclerosis [34] and may be a future option in CKD [35] or forms of cancer [36]. According to our results, selective ETB antagonism with biologicals, which is under development [1], may, at first glance, be an option to prevent or to ameliorate manifestations of metabolic syndrome, in particular glucose intolerance/type 2 diabetes, obesity, and hypertriglyceridemia. Dual ETA/ETB antagonism with bosentan has similarly proven effective to ameliorate glucose intolerance [15], but how bosentan accomplishes this has remained unclear. Our study demonstrated that ETB deficiency causes enhanced production of T3/FGF21, resulting in higher energy expenditure. Although this mechanism can definitely be expected to favorably impact metabolic syndrome, it may include the risk of adverse effects of hyperthyroidism which are well characterized. This might definitely be a serious limitation of the use of ETB antagonism in metabolic syndrome. Therefore, further studies are needed to define the advantage and possible side effects of ETB antagonism in humans for metabolic disease.

Taken together, ETB-deficient mice were protected from metabolic syndrome characterized by glucose intolerance, WAT accumulation, and hypertriglyceridemia induced by HFD feeding compared to wild type mice. The protection was, at least in part, dependent on higher levels of T3 and FGF21 resulting in higher energy expenditure in ETB deficiency.

## AUTHOR CONTRIBUTIONS

MFe, BH, CW, and MFö designed the research. MFe and MFö interpreted data. MFe and MFö wrote the manuscript; MFe, LM, JS, MH, JV, AW, SH, and MJK performed research and analyses. All authors read and approved the final manuscript.

## ACKNOWLEDGEMENTS

We thank C. Heidel, H. Fross, A. Ullrich, and M. Radtke for technical help and Prof. Donatus Nohr for histology support. This study was supported by Deutsche Forschungsgemeinschaft (DFG, grant # Fo695/2–2).

## DECLARATION OF COMPETING INTEREST

The authors declare the following financial interests/personal relationships which may be considered as potential competing interests: Michael Foeller reports financial support was provided by Deutsche Forschungsgemeinschaft (German Research Foundation), a non-profit organization.

## DATA AVAILABILITY

Data will be made available on request.

 

## APPENDIX A. SUPPLEMENTARY DATA

Supplementary data to this article can be found online at https://doi.org/10.1016/j.molmet.2023.101868.

## REFERENCES


[1] Dhaun N, Webb DJ. Endothelins in cardiovascular biology and therapeutics. Nat Rev Cardiol 2019;16:491–502.

[2] Maguire JJ, Davenport AP. Endothelin receptors and their antagonists. Semin Nephrol 2015;35:125–36.

[3] Schneider MP, Boesen EI, Pollock DM. Contrasting actions of endothelin ET(A) and ET(B) receptors in cardiovascular disease. Annu Rev Pharmacol Toxicol 2007;47:731–59.

[4] Boyen GBT von, et al. Abnormalities of the enteric nervous system in heterozygous endothelin B receptor deficient (spotting lethal) rats resembling intestinal neuronal dysplasia. Gut 2002;51:414–9.

[5] Quaschning T, et al. Endothelin B receptor-deficient mice develop endothelial dysfunction independently of salt loading. J Hypertens 2005;23:979–85.

[6] Feger M, Ewendt F, Menzel M, Hocher B, Föller M. Endothelin receptor B controls the production of fibroblast growth factor 23. Faseb J 2020;34:6262–70.

[7] Kelland NF, et al. Endothelial cell-specific ETB receptor knockout: autoradiographic and histological characterisation and crucial role in the clearance of endothelin-1. Can J Physiol Pharmacol 2010;88:644–51.

[8] Ivy D, et al. Endothelin B receptor deficiency potentiates ET-1 and hypoxic pulmonary vasoconstriction. Am J Physiol Lung Cell Mol Physiol 2001;280:L1040–8.

[9] Kohan DE, Pollock DM. Endothelin antagonists for diabetic and non-diabetic chronic kidney disease. British Journal of Clinical Pharmacology 2013;76(4):573–9.

[10] Saklayen MG. The global epidemic of the metabolic syndrome. Curr Hypertens Rep 2018;20:12.

[11] Vernia S, et al. Phosphorylation of RXRα mediates the effect of JNK to suppress hepatic FGF21 expression and promote metabolic syndrome. Proc Natl Acad Sci USA 2022;119:e2210434119.

[12] Camporez JPG, et al. Cellular mechanisms by which FGF21 improves insulin sensitivity in male mice. Endocrinology 2013;154:3099–109.

[13] Schlein C, et al. FGF21 lowers plasma triglycerides by accelerating lipoprotein catabolism in white and Brown adipose tissues. Cell Metabol 2016;23:441–53.

[14] Straub L, Wolfrum C. FGF21, energy expenditure and weight loss - how much brown fat do you need? Mol Metabol 2015;4:605–9.

[15] Rivera-Gonzalez O, Wilson NA, Coats LE, Taylor EB, Speed JS. Endothelin receptor antagonism improves glucose handling, dyslipidemia, and adipose tissue inflammation in obese mice, vol. 135. London, England: Clinical science; 2021. p. 1773–89. 1979.

[16] Rivera-Gonzalez OJ, Kasztan M, Johnston JG, Hyndman KA, Speed JS. Loss of endothelin type B receptor function improves insulin sensitivity in rats. Can J Physiol Pharmacol 2020;98:604–10.

[17] Tabeling C, et al. Endothelin B receptor immunodynamics in pulmonary arterial hypertension. Front Immunol 2022;13:895501.

[18] Tschöp MH, et al. A guide to analysis of mouse energy metabolism. Nat Methods 2011;9:57–63.

[19] Chu C-H, et al. Hyperthyroidism is associated with higher plasma endothelin-1 concentrations. Exp Biol Med 2006;231:1040–3.

[20] Juergens UR, et al. Inflammatory responses after endothelin B (ETB) receptor activation in human monocytes: new evidence for beneficial anti-inflammatory potency of ETB-receptor antagonism. Pulm Pharmacol Therapeut 2008;21:533–9.

[21] Wilson SH, Simari RD, Lerman A. The effect of endothelin-1 on nuclear factor kappa B in macrophages. Biochem Biophys Res Commun 2001;286:968–72.

[22] Kleiner S, et al. Development of insulin resistance in mice lacking PGC-1α in adipose tissues. Proc Natl Acad Sci USA 2012;109:9635–40.

[23] Shoelson SE, Lee J, Goldfine AB. Inflammation and insulin resistance. J Clin Invest 2006;116:1793–801.

[24] Meidan E, Kolesnikov Y, Tirosh O. High fat diets composed of palm stearin and olive oil equally exacerbate liver inflammatory damage and metabolic stress in mice. Mol Nutr Food Res 2018;62:e1700915.

[25] Cyphert HA, Alonge KM, Ippagunta SM, Hillgartner FB. Glucagon stimulates hepatic FGF21 secretion through a PKA- and EPAC-dependent posttranscriptional mechanism. PLoS One 2014;9:e94996.

[26] Badman MK, et al. Hepatic fibroblast growth factor 21 is regulated by PPARalpha and is a key mediator of hepatic lipid metabolism in ketotic states. Cell Metabol 2007;5:426–37.

[27] Kharitonenkov A, et al. FGF-21 as a novel metabolic regulator. J Clin Invest 2005;115:1627–35.

[28] Adams AC, et al. Thyroid hormone regulates hepatic expression of fibroblast growth factor 21 in a PPARalpha-dependent manner. J Biol Chem 2010;285:14078–82.

[29] Reddy P, Lent-Schochet D, Ramakrishnan N, McLaughlin M, Jialal I. Metabolic syndrome is an inflammatory disorder: a conspiracy between adipose tissue and phagocytes. Clinica chimica acta; international journal of clinical chemistry 2019;496:35–44.

[30] Sampaio AL, Rae GA, D'Orléans-Juste P, Henriques MG. ETA receptor antagonists inhibit allergic inflammation in the mouse. J Cardiovasc Pharmacol 1995;26(3):S416–8.

[31] Wang H, Ye J. Regulation of energy balance by inflammation: common theme in physiology and pathology. Rev Endocr Metab Disord 2015;16:47–54.

[32] Wilde DW, Massey KD, Walker GK, Vollmer A, Grekin RJ. High-fat diet elevates blood pressure and cerebrovascular muscle Ca(2+) current. Hypertension (Dallas, Tex. : 1979 2000;35:832–7.

[33] Dupuis J, Hoeper MM. Endothelin receptor antagonists in pulmonary arterial hypertension. Eur Respir J 2008;31:407–15.

[34] Huh J, Black L, Blasio DC de, Tracy CL, Berry-Cabán CS. Novel use of bosentan for postoperative wound healing of the foot in systemic sclerosis. J Clin Rheumatol : Practical Reports on Rheumatic & Musculoskeletal Diseases 2021;27:S692–3.

[35] Raina R, et al. The role of endothelin and endothelin antagonists in chronic kidney disease. Kidney Dis 2020;6:22–34.

[36] Voutouri C, et al. Endothelin inhibition potentiates cancer immunotherapy revealing mechanical biomarkers predictive of response. Adv Ther 2021;4:2000289.


 